# Global zoogeography of fragile macrozooplankton in the upper 100–1000 m inferred from the underwater video profiler

Lars Stemmann, Marsh Youngbluth, Kevin Robert, Aino Hosia, Marc Picheral, Harriet Paterson, Frederic Ibanez, Lionel Guidi, Fabien Lombard, and Gabriel Gorsky

Stemmann, L., Youngbluth, M., Robert, K., Hosia, A., Picheral, M., Paterson, H., Ibanez, F., Guidi, L., Lombard, F., and Gorsky, G. 2008. Global zoogeography of fragile macrozooplankton in the upper 100–1000 m inferred from the underwater video profiler. – ICES Journal of Marine Science, 65: 433–442.

Mesopelagic gelatinous zooplankton fauna are insufficiently known because of inappropriate and infrequent sampling, but may have important trophic roles. *In situ* imaging systems and undersea vehicles have been used to investigate their diversity, distribution, and abundance. The use of different platforms, however, restricts the comparison of data from different regions. Starting in 2001, the underwater video profiler (UVP) was deployed during 12 cruises in six oceanic regimes (Mediterranean Sea, North Atlantic shelves, Mid-Atlantic Ridge, tropical Pacific Ocean, eastern Indian Ocean, and Subantarctic Ocean) to determine the vertical distribution of organisms in the upper 1000 m. Nine oceanic regions were identified based on the hydrological properties of the water column. They correspond to nine of the biogeochemical provinces defined by Longhurst. In all, 21 morphotypes were recognized: sarcodines (eight groups), ctenophores (two groups), siphonophores, medusae (five groups), crustaceans (one group), chaetognaths, appendicularians, salps, and fish. The similarity in the community assemblages of zooplankton in the 100–1000 m layer was significantly greater within regions than between regions, in most cases. The regions with comparable composition were located in the North Atlantic with adjacent water masses, suggesting that the assemblages were either mixed by advective transport or that environmental conditions were similar in mesopelagic layers. The data suggest that the spatial structuring of mesopelagic macrozooplankton occurs on large scales (e.g. basin scales) but not necessarily on smaller scales (e.g. oceanic front).

**Keywords:** biogeochemical province, gelatinous zooplankton, mesopelagic, underwater video profiler, zoogeography.

Received 11 July 2007; accepted 30 November 2007; advance access publication 5 March 2008.

*L. Stemmann, K. Robert, F. Ibanez, L. Guidi, and F. Lombard: Université Pierre et Marie Curie-Paris 6, UMR 7093, Villefranche sur Mer F-06234, France. L. Stemmann, M. Picheral, F. Ibanez, and G. Gorsky: Laboratoire d'Océanographie de Villefranche (LOV), BP 28, 06234 Villefranche sur Mer Cedex, France. H. Paterson: School of Environmental Systems Engineering, University of Western Australia, Western Australia, Australia. A. Hosia: Department of Biology, University of Bergen, PO Box 7800, N-5020 Bergen, Norway. M. Youngbluth: Harbor Branch Oceanographic Institution, 5600 US 1 North, Fort Pierce, FL 34946, USA. Correspondence to L. Stemmann: tel: +33 493763811; fax: +33 493763834; e-mail: stemmann@obs-vlr.fr*

## Introduction

The zoogeography and spatial distribution of fragile midwater zooplankton (e.g. sarcodines, ctenophores, cnidarians, and tunicates) are basically unknown because they cannot be sampled adequately with plankton nets (Robison, 2004; Vinogradov, 2005). Direct observation and collection of these fauna from manned and unmanned vehicles have documented their *in situ* behaviour, taxonomic diversity, spatial distribution, and relative abundance. Imaging systems also allowed quantification of zooplankton over scales of centimetres to kilometres. Data obtained with these different optical approaches are difficult to compare across regions because observational techniques and fields of view vary. Most investigations have focused on the diversity and behaviour of relatively large (a few centimetres to metres) fauna (Raskoff, 2001; Lindsay *et al.*, 2004; Lindsay and Hunt, 2005). The quantification of small (millimetres to centimetres) organisms, lumped into higher taxonomic groups, has also been pursued (Stemmann *et al.*, 2008). As a consequence, the zoogeography of the midwater fauna remains unclear, and this paper presents the first comparisons of mesopelagic assemblages conducted across oceanic regions using a single imaging technology and a consistent deployment technique.

In an attempt to understand the balance between pelagic production and consumption, Longhurst (1998) partitioned the global ocean into a number of distinct biogeochemical provinces that could be differentiated by epipelagic criteria such as "ocean currents, fronts, topography, and recurrent features in the sea surface chlorophyll field". He hypothesized that assemblages of organisms from different locations within a defined biogeochemical province would be more similar to each other than those from different provinces. The establishment of association between biogeochemical and zoogeographic patterns would provide support

for the division of the global ocean into functionally distinct provinces in the upper 1000 m of the ocean.

The first objective of this study is to present quantitative assessments of the vertical (0–1000 m) distributions of gelatinous and other macrozooplankton (>1 cm) in nine regions of six oceanic basins (Mediterranean Sea, North Atlantic shelves, Mid-Atlantic Ridge, tropical Pacific Ocean, eastern Indian Ocean, and Subantarctic Ocean). The second objective is to assess the degree of association between midwater macrozooplankton assemblages and the main epipelagic biogeochemical provinces.

## Methods

### Sampling sites

The vertical distribution of major groups of macrozooplankton in different oceanic basins was observed at 296 stations (12 cruises) with the underwater video profiler (UVP; see Table 1; Figure 1). Three cruises took place in the North Atlantic Ocean in October and November 2001 (POMME 3 cruises, 77 stations), in September 2002 (MAINE 2002 cruise, 54 stations), and June–July 2004 (MARECO 2004 cruise, 36 stations). One cruise was conducted in Norwegian fjords during November 2002 (MARECO 2002 cruise, ten stations). Four cruises were conducted in the northwest Mediterranean Sea at the French JGOFS time-series station in March, May, and June 2003 (18 stations), and in September 2006 (OIM cruise, six stations). One cruise took place along a section across the South Pacific Gyre in November 2004 (BIOSOPE cruise, 76 stations). The KEOPS cruise was conducted in January–February 2005 around the Kerguelen Island in the Subantarctic Ocean (25 stations). Finally, the SS05 2006 cruise was completed in the eastern boundary of the Indian Ocean in May 2006 (29 stations).

Examination of the temperature and salinity profiles in the upper 1000 m during the 12 cruises identified nine regions with similar TS properties (Figure 2). The Mediterranean region was characterized by the highest midwater salinity and temperature of the Mediterranean intermediate water (MIW). The section in the South Pacific Gyre crossed typical South Pacific intermediate water (SPIW). The SS0506 cruise traversed an anticyclonic eddy of water from the Leeuwin Current. The Subantarctic region had low salinity and the coldest water. In the North Atlantic, four regions were defined following the grouping of Stemmann *et al.* (2008). The first region, characterized by Subarctic intermediate water (SAIW), was sampled only during the MARECO 2004 cruise and had the lowest temperature and salinity within the 100–1000 m layer. This water mass is typical for the area between the edge of the Greenland coastal current and the Subpolar Front (SPF). The second region was identified as North Atlantic central water (NACW) and was sampled during the MARECO 2004 and the POMME 3 cruises. This water mass had the highest temperature and salinity in the North Atlantic. This water mass is bounded to the west and northwest by the eddy field of the Gulf Stream and to the northeast by the bifurcation of the flow between the Azores Current and the North Atlantic Drift, that is, at ~40–42°N. The third region was characterized by intermediate TS properties in the upper 1000 m and corresponded to Modified North Atlantic Water (MNAW). This water mass is part of the westward flow of Atlantic water along

**Table 1.** List of the cruises sampled by the UVP from 2001.

| Cruise | Date | Number of profiles | Location/main intermediate water mass | Biogeochemical provinces |
|---|---|---|---|---|
| OIM2006[a] and Barmed[b] | September 2006 | 8 | Northwest Mediterranean Sea/ MIW | Mediterranean Sea (MEDI) |
| | March–June 2003 | 18 | | |
| BIOSOPE[c] | November 2004 | 35 (76) | South Pacific Gyre/SPIW | South Pacific Subtropical Gyre (SPSG) |
| KEOPS[d] | January–February 2005 | 8 (25) | West of Kerguelen Islands | Subantarctic Ocean (SANT) |
| Maine2002 | September 2002 | 0 (54) | Canyons south of Georges Bank | Northwest Atlantic shelves (not used in the global analysis) |
| MARECO[e] | June–July 2004 | 12 | North Atlantic Subpolar Gyre/ NACW | North Atlantic Subtropical Ocean (NAST) |
| | | 15 | North Atlantic Polar Gyre/SAIW | Atlantic Arctic (ARCT) |
| | | 3 | Northeast Atlantic/MNAW | Atlantic Subarctic (SARC) |
| | | 6 | North Atlantic SPF/North Atlantic Current | North Atlantic drift (NADR) |
| MARECO 2002 | November 2002 | 10 | Norwegian fjord | Northeast Atlantic shelves (NECS) |
| POMME[f] 3 (2 cruises) | October–November 2001 | 39 (41) | North Atlantic Subpolar Gyre/ NACW | North Atlantic Subtropical (NAST) |
| SS052006[g] | May 2006 | 29 | Eastern boundary waters of the Indian Ocean | Western Australia (AUSW) |

In the third column, the number in parentheses indicates the total number of profiles that were performed during each cruise, whereas the number of profiles used in the statistical analysis is indicated in front of parentheses (see text). The names of the biogeochemical provinces are given (Longhurst, 1998) in the last column.

[a]Océanographie, Instrumentation et Methodologie cruise.
[b]Barium in the Mediterranean Sea programme.
[c]Biogeochemistry and Optics South Pacific Experiment cruise.
[d]Kerguelen: compared study of the Ocean and the Plateau in Surface water cruise.
[e]Mid-Atlantic Ridge ECOsystem programme.
[f]Programme Océan Multidisciplinaire Méso Echelle.
[g]Southern Surveyor voyage.

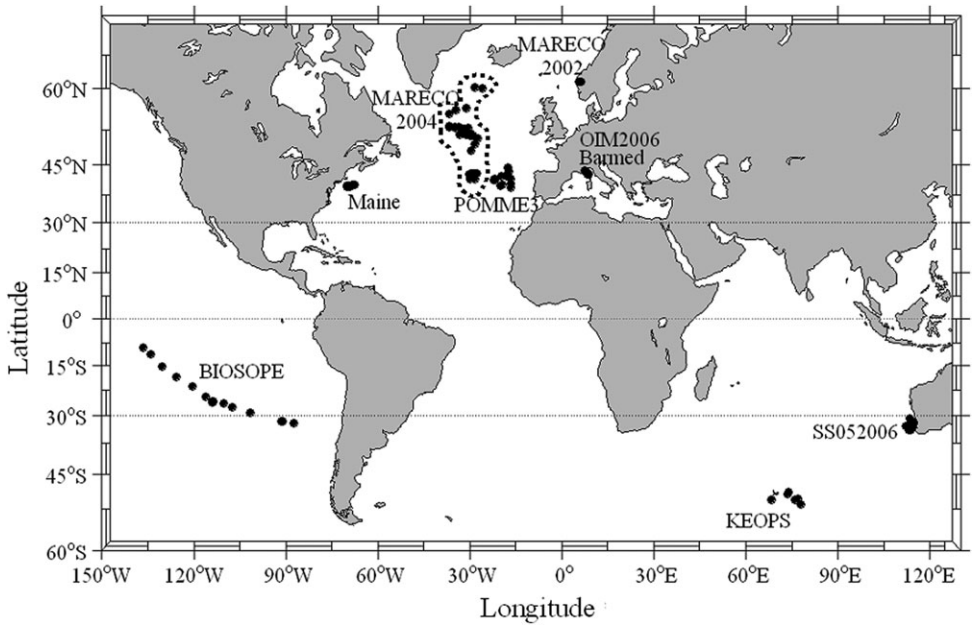


**Figure 1.** The area and stations sampled during the different cruises. The dotted line identifies the station performed during the MARECO 2004 cruise.

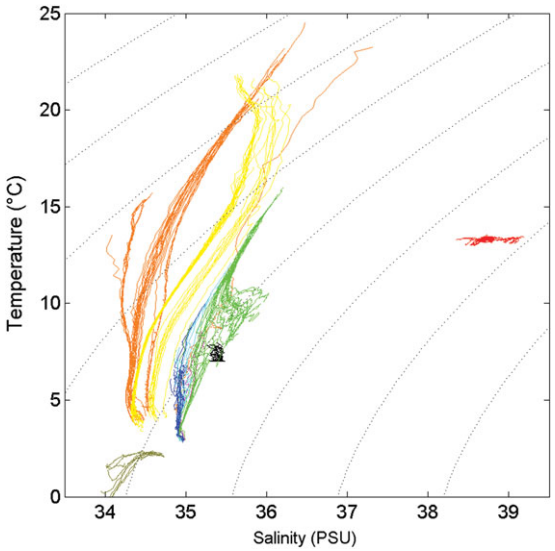


**Figure 2.** Temperature–salinity diagrams of all the vertical profiles. The colour coding is the following: MEDI (red), NAST (green), NADR (light blue), SARC (magenta), ARCT (dark blue), NECS (black), SANT (brown), SPSG (orange), and AUSW (yellow).

the Reykjanes Ridge. The fourth region of the North Atlantic consisted of the profiles that were performed in the SPF area during the MARECO cruise in the front and in an eddy. The profiles were separated in Stemmann *et al.* (2008), but the data are combined here because no significant differences in the zooplankton community were detected by Stemmann *et al.* (2008). The water mass in the Norwegian fjords had TS properties distinct from the other water mass of the North Atlantic. Although based solely on the TS properties and the knowledge of the oceanic circulation during each cruise, the nine regions defined in this study correspond to nine of the biogeochemical provinces defined by Longhurst (1998; Table 1). Therefore, they are distinguished using Longhurst's nomenclature.

## UVP deployments and macrozooplankton identification

The UVP enumerates and measures macrozooplankton (>0.5 mm), as well as particle aggregates (>60 μm) such as marine snow (Gorsky *et al.*, 2000). The lighting system consists of two 54W Chadwick Helmuth stroboscopes synchronized with two video cameras (resolution = 732 × 570 pixels), one with a 25 mm (narrow angle) and the other with an 8 mm (wide angle) lens. Four mirrors spread the strobe-light beams into a structured 8 cm thick slab. The short flash duration (pulse duration = 30 μs) allows the UVP to descend relatively rapidly (up to 1.5 m $s^{-1}$) without deterioration of image quality. The volumes illuminated for each images are 1.3 l and 10.5 l, respectively, and they are recorded simultaneously at 12 Hz. The two cameras are positioned perpendicular to the light slab, so that only objects illuminated against a dark background are recorded. The UVP does not alter the water in the field of view because only images in front of the frame are recorded during the downcast. Each cast to 1000 m provides ~12 000 images per camera. A camera equipped with a wide-angle lens was used to quantify the abundance of macrozooplankton surveys ~120 $m^3$ for a 0–1000 m cast. Depth, temperature, and conductivity data are acquired simultaneously with a Seabird Seacat 19 CTD probe (S/N 1539), together with estimates of Chl *a* and particle mass using a fluorometer and a nephelometer (both from Chelsea Instruments Ltd). These data are stored in ASCII files.

All profiles were analysed using the same protocol. Images from the wide-angle camera are automatically screened with a custom software routine to extract objects larger than 100 pixels (ca. 0.5 mm) with a mean grey level of 28. Most of the organisms

cannot be identified below that size because of the low resolution of the image. This configuration was chosen as an optimal compromise between obtaining a limited number of objects to analyse (<2000) and the reliable detection of small and transparent organisms after many tests. About 5–10% of these images contain interesting targets, which were visually reviewed to identify taxa. The complete analysis of a profile takes ~2 h. Among the 329 available profiles, only 183 were included in the statistical analysis. The remaining 146 were excluded because they only reached 500 or 700-m depth (105 profiles), or the image treatment could not follow the standard protocol because the number of images extracted was too high (>50 000) with a size cut-off at 100 pixels.

## Macrozooplankton groups included in the analyses

Macrozooplankton were lumped into 21 major groups, because identification to lower taxonomic levels was not possible. This procedure maximized the number of individuals per group and allowed statistical comparisons of groups in each oceanic region. The organisms identified were 1–10 cm long, except for the single-celled sarcodines (<1 cm; Figure 3). Sarcodines were divided into eight groups. The first group had a characteristic morphology with a central disc (up to 0.5 cm) and several tentacles (mostly four); sometimes their tentacles attached two individuals. These were identified as radiolaria of suborder Phaeodaria (Haeckel, 1887; hereafter Phaeo.). The second group had typical radial spines (Spine.). The third group was similar to the Spine., but the individuals were attached in pairs (Spine2.). The fourth group had more hair-like spines (Stars.), the fifth had groups of four attached cells (RadioCS.), and the sixth showed a spherical kernel surrounded by a halo (Sphere.). The two remaining groups were colonial. The seventh group had flat, cylindrical colonies (RadioC.), whereas the eighth also had flat, cylindrical colonies but was ramified (RadioCD.). The ctenophores were divided into two groups: cydippids (Cyd.) and lobates (Lob.). The siphonophores (Siph.) were pooled into a single group because the resolution of the images did not always allow calycophorans to be distinguished from physonects. Five groups of medusae were formed: the trachymedusae *Aglantha* spp. (Agl.) and *Haliscera* spp. (Hal.), the narcomedusae *Aeginura grimaldii* (Gri.) and *Solmundella bitentaculata* (Sol.), and "other medusae" (Med., which included other hydromedusae as well as all scyphomedusae).

Crustaceans (Crust.) included amphipods, large decapods, euphausiids, and other crustaceans that could not be categorized because of poor image quality. Copepods were excluded from analyses because they were usually too small for quantitative assessments. All chaetognaths (Chaet.) were pooled. Tunicates were subdivided into two groups: appendicularians (App.), encompassing fritillarians and oikopleurids, and thaliaceans (Thal.), which included doliolids and salps, salps being numerically dominant. The fish (Fish) were lumped into one group although different families or genera could be identified (e.g. *Cyclothone*).

## Numerical analysis

The numerical analysis of the zooplankton data included five steps. (i) Vertical binning of each profile, (ii) assessment of diel vertical migration (DVM) to justify pooling day and night data, (iii) objective assessment of variability in the community structure, using multidimensional-scaling (MDS; Clarke and Warwick, 2001)

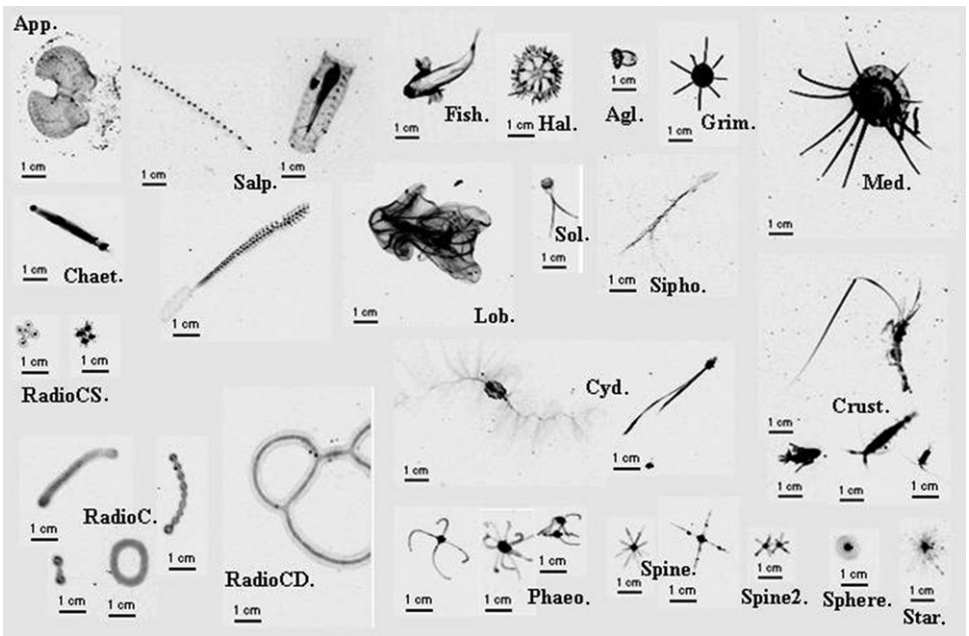


**Figure 3.** UVP video images of individuals from each of the macrozooplankton groups analysed; appendicularians (App.), Thaliacae (Thal.; salp and doliolid), Fish, *Haliscera* spp. medusa (Hal.), *S. bittentaculata* (Sol.), *Aglantha* spp. (Agl.), *Aeginura grimaldii* (Gri.), and "other medusae" (Med.), chaetognath (Chaet.), lobate ctenophore (Lob.), cydippid ctenophore (Cyd.), siphonophore (Siph.), crustaceans (Crust.; decapod and amphipod), single-cell sarcodine grouped by four (RadioCS.), colonial radiolarians (RadioC.), colonial radiolarians with double line (RadioCD.), Phaedorian (Phaeo.), single-cell sarcodine with spines (Spine.), double-cell sarcodine with spines (Spine2.), spheres (Sphere.), and sarcodine with hairs (Stars.). The scale bar represents approximately 1 cm. Additional images can be viewed at http://www.obs-vlfr.fr/LOV/ZooPart/Gallery/.

analysis, (iv) ANOSIM procedure (Clarke and Warwick, 2001) to assess the significance of the within-oceanic region variability against the among-regions variability, and (v) assembling profiles by oceanic regions.

Each step is described as follows. (i) The abundance of each group was binned in 100 m layers from 0 to 1000 m, yielding a sample volume of 12 $m^3$ per depth interval for each profile. (ii) DVM was tested for with a Monte Carlo procedure (Perry and Smith, 1994). The empirical cumulative distribution functions (cdfs) of the vertical distribution of each macrozooplankton group were calculated for the available day and night profiles in each region. The statistical analysis was similar to the empirical cdfs in Kolmogorov–Smirnov tests. The maximum absolute vertical distance between the two cdfs was calculated and compared with the distribution obtained with a Monte Carlo resampling of the data (Legendre and Legendre, 1998). (iii) The MDS displays the relative similarity between samples as the distance between points in two-dimensional space. Thus, tightly grouped samples are very similar, whereas more dispersed samples are more different, thereby providing a visual representation of gradual changes. The MDS was performed on concentrations of macrozooplankton integrated over a 100–1000 m interval. The abundances were second-root transformed to decrease the importance of numerically dominant groups, and a matrix of Bray–Curtis similarities between samples was constructed. (iv) The ANOSIM test was performed on the same Bray–Curtis similarities between samples matrix-grouped into the nine oceanic regions. (v) The average and standard deviation of abundance vertical profiles were calculated for each region.

## Results

### Relative importance of each taxa

More than 5000 organisms were identified in the 100–1000-m depth layer (Figure 4). The numerically dominant groups were crustaceans (24%) followed by the medusae (18% pooled Med., Agl., Hal., Sol., and Gri.), appendicularians (14%), chaetognaths (11%), fish (7%), and single-cell sarcodines of the Star. group (6%; Figure 4). The other taxonomic groups made up <5% of the total count each. However, the pooling of all single-cell sarcodines made this group rank second (23%).

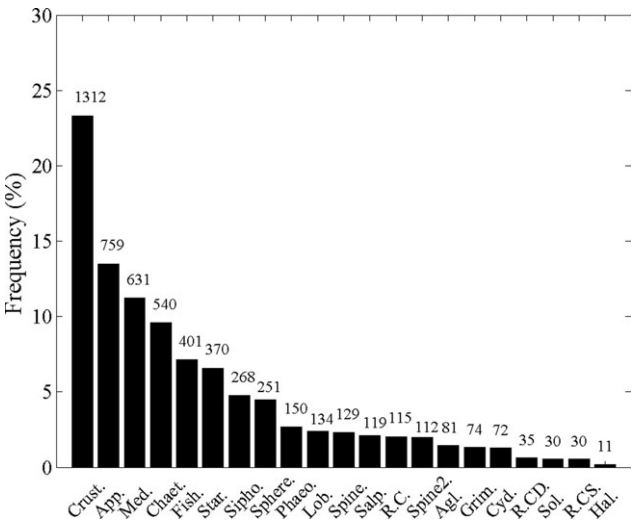


**Figure 4.** Frequency of occurrence for the different macrozooplankton groups calculated from the 183 profiles. The total number of individuals is noted at the top of each column.

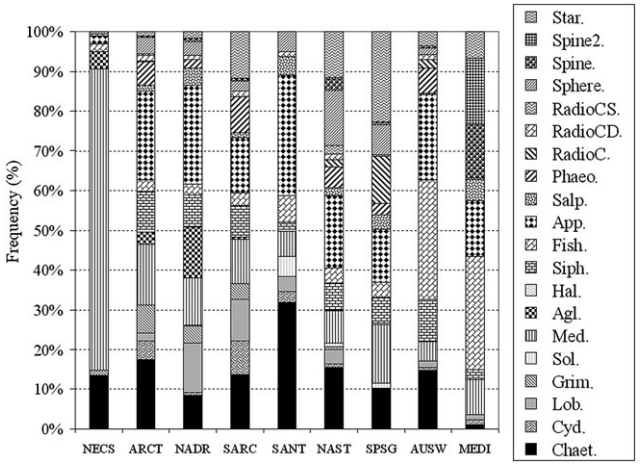


**Figure 5.** Frequency of occurrence of the 21 taxonomic groups in the nine regions. The order of the region is set so that the proportion of carnivorous organisms (all in grey from Chaet. to Siph.) decreases from left to right.

From a trophic perspective, the assemblages of zooplankton could be lumped into three categories (Figure 5): gelatinous carnivores (Cyd., Lob., Med., Siph., and Chaet.), filter-feeder detritivores (App. and Salp.), and omnivores (Sarc., Crust., and fish). Interestingly, the proportion of carnivores decreased from 95% to 15%, from the high-latitude regions (NECS, ARCT, NADR, SARC, and SANT) to the low-latitude regions (MEDI, AUSW, and SPSG).

### Statistical analyses of macrozooplankton distributions

The test for DVM revealed no significant differences in the vertical distributions between day and night for any of the macrozooplankton groups except euphausiids. The latter group was excluded from the MDS and ANOSIM analysis.

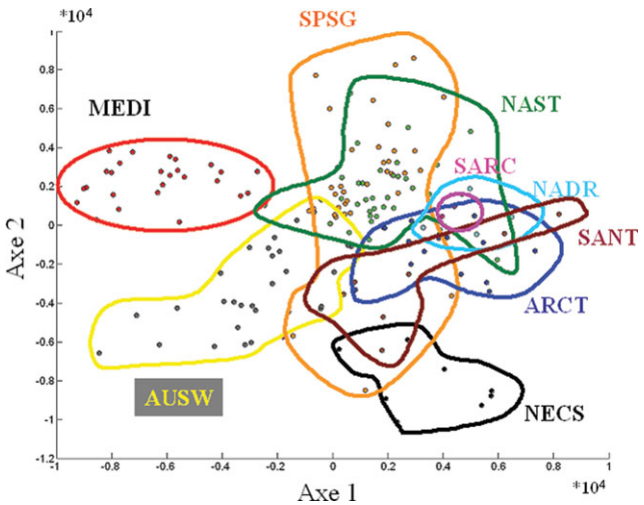


**Figure 6.** Results from MDS of the spatial zooplankton community structure defined in the 183 UVP profiles (stress: 0.28). Encircled groups correspond to the nine regions defined by the water-mass analysis. The colour coding is the same as for Figure 2, except for the AUSW regions, which are set to grey for better visualization.

**Table 2.** ANOSIM test statistic *R*-values (lower diagonal) and probability of accepting the null hypothesis that regions are similar (upper diagonal) of pairwise comparison of each region.

| | MEDI | SPSG | SANT | NECS | SARC | ARCT | NAST | NADR | AUSW |
|---|---|---|---|---|---|---|---|---|---|
| **MEDI** | X | $p < 0.001$ | $p < 0.001$ | $p < 0.001$ | $p < 0.001$ | $p < 0.001$ | $p < 0.001$ | $p < 0.001$ | $p < 0.001$ |
| **SPSG** | 0.84 | X | $p < 0.001$ | $p < 0.001$ | $p = 0.007$ | $p < 0.001$ | $p < 0.001$ | $p < 0.001$ | $p < 0.001$ |
| **SANT** | 0.974 | 0.64 | X | $p < 0.001$ | $p = 0.0167$ | $p < 0.001$ | $p < 0.001$ | $p = 0.0012$ | $p < 0.001$ |
| **NECS** | 0.998 | 0.848 | 0.903 | X | $p = 0.0061$ | $p < 0.001$ | $p < 0.001$ | $p < 0.001$ | $p < 0.001$ |
| **SARC** | 0.987 | 0.615 | 0.527 | 0.97 | X | $p = 0.2328$ | $p = 0.027$ | $p = 0.1548$ | $p = 0.006$ |
| **ARCT** | 0.985 | 0.589 | 0.705 | 0.949 | 0.130* | X | $p < 0.001$ | $p = 0.006$ | $p < 0.001$ |
| **NAST** | 0.872 | 0.245 | 0.608 | 0.972 | 0.387 | 0.445 | X | $p < 0.001$ | $p < 0.001$ |
| **NADR** | 0.984 | 0.603 | 0.73 | 0.937 | 0.197* | 0.3 | 0.4 | X | $p < 0.001$ |
| **AUSW** | 0.841 | 0.554 | 0.592 | 0.847 | 0.562 | 0.668 | 0.642 | 0.802 | X |

The global $R = 0.6792$, $p < 0.001$ (1000 on 7.52E + 131 possible permutations). Non-significant ($p > 0.05$) pairwise comparisons are indicated by asterisk.

The MDS plot (Figure 6) revealed that five of the nine regions were clearly different from each other in their taxonomic composition (MEDI, AUSW, NECS, ARCT, and SPSG). The other regions more or less overlap such that the pattern is less consistent based on the MDS plot. The stress value is relatively high, reflecting the variability in the dataset. The variability in the taxonomic composition may be the result of natural spatial variability and/or more probably, the rather small volume of water used to assess the macrozooplankton distribution.

The analysis of the global R statistics by the ANOSIM demonstrated that the differences in the macrozooplankton communities between regions were significantly greater than within regions. In addition, pairwise comparisons of the macrozooplankton communities between regions clearly indicated that all regions were different from each other, except for the SARC region with respect to the ARCT and NADR regions (Table 2).

## Spatial and vertical distribution of selected taxa

The spatial distribution, based on concentrations integrated over the 0–1000-m depth interval, is shown in Figure 7, and their average vertical distribution in each region is reported in Figures 8 and 9.

The Phaeodorians were found in each region except the MEDI, NECS, and SANT regions. This group was always mesopelagic, except in two regions (SARC and AUSW), where they occurred at 100 m. The maximum concentration exceeded 20 ind. 100 $m^{-3}$ in the NAST region. Medusae were the most abundant group of soft-bodied zooplankton (pooling Med., Agl., Hal., Sol., and Gri.) and were generally many at all stations in all regions. Maxima of 10 000 ind. $m^{-2}$ were observed in the Norwegian fjords. Up to 40 ind. 100 $m^{-3}$ were recorded in the NECS region at depths >500 m. Chaetognaths occurred in all regions with concentrations up to 15 ind. 100 $m^{-3}$. The lowest abundance of chaetognaths was found in the MEDI region. Vertical distributions differed between regions. This group occurred below 400 m in the NECS, NAST, and NADR, but was homogeneously distributed throughout the water column in the other regions. Appendicularians were consistently many at all stations in all regions. Maxima of 10 000 ind. $m^{-2}$ were observed in different regions (NADR and NECS). Their maximum vertical

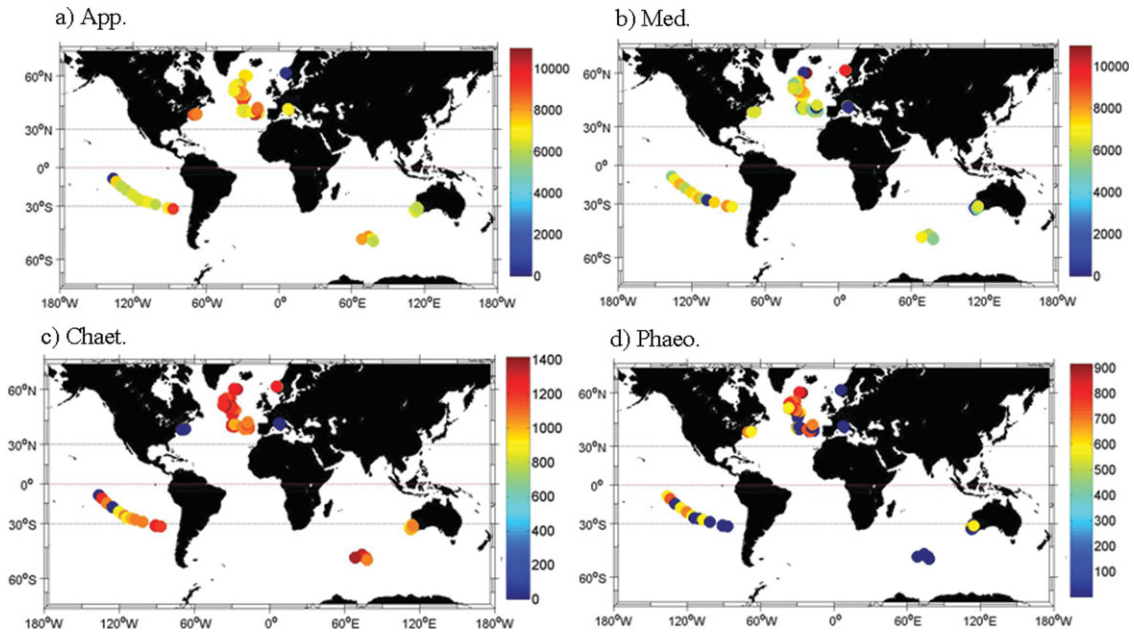


**Figure 7.** Maps of abundance (ind. $m^{-2}$) of selected macrozooplankton groups.

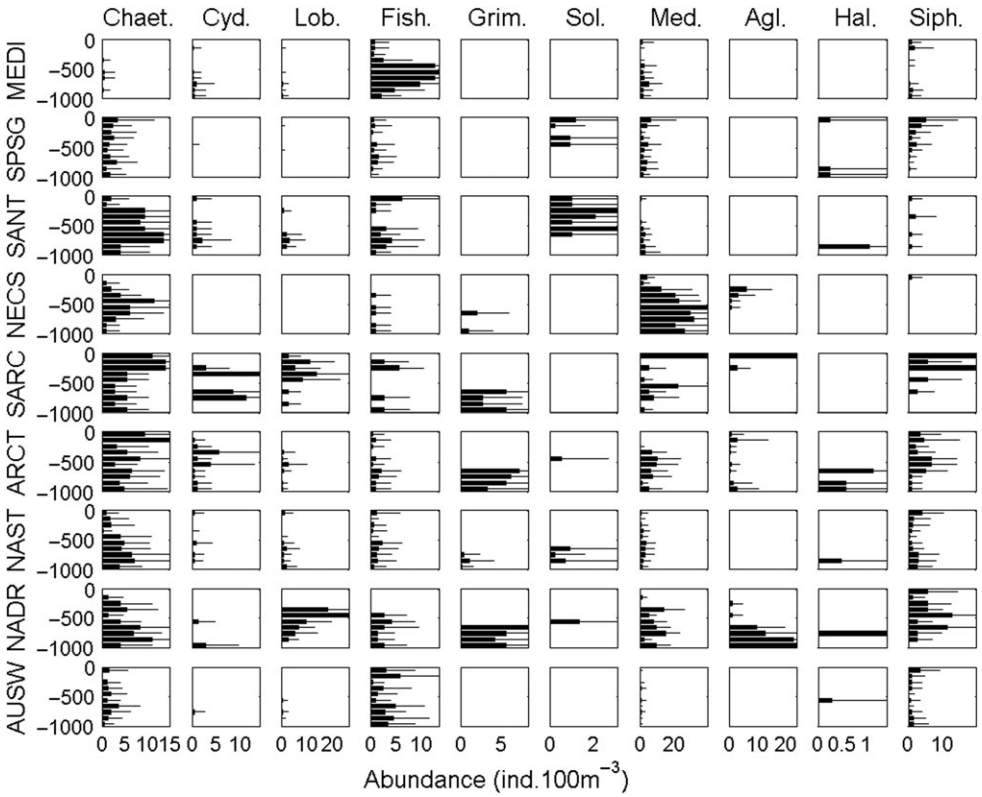


**Figure 8.** Vertical distribution of macrozooplankton in the different water masses. Average abundance (horizontal bars) and standard deviation (error bars) are noted for the following groups: chaetognaths (Chaet.), cydippids (Cyd.), lobates (Lob.), fish, *Aeginura grimaldii* (Gri.), *S. bitentaculata* (Sol.), "other medusae" (Med.), *Aglantha* spp. (Agl.), *Haliscera* spp. (Hal.), and siphonophores (Siph.) in the nine regions (rows).

concentration (up to 58 ind. 100 m$^{-3}$) was between 300 and 400 m in the NADR region. However, epipelagic populations of smaller individuals (up to 10 ind. m$^{-3}$) were observed in the NAST and AUSW regions. Appendicularians were rare in the NECS region.

In the MDS representation, the MEDI and NEC regions are clearly different from each other. The major difference comes from the large decrease in gelatinous predators in the MEDI region compared with the NECS region (from 95% to 15%; Figure 5). This decrease is the result of the large increase in abundances of mesopelagic fish and sarcodines in the MEDI (maximum of 15 and 10 ind. 100 m$^{-3}$) relative to the NECS region, where they are almost absent (Figures 8 and 9). These two groups are replaced in the mesopelagic layer of NECS by chaetognaths and medusae (Figure 8). In the MDS representation, the SPSG and NAST regions overlap, although they are significantly different in the ANOSIM test. These two regions have similar and large proportions of sarcodines (40%). However, a more detailed analysis of the sarcodine groups reveals that they are different. Spines., RadioCD., and RadioCS. dominate in the NAST region, whereas they are nearly absent from SPSG region (Figure 9).

## Discussion

Zoogeographic studies tend to be based on presence–absence data, because they rely heavily on historical literature to support distribution patterns. These records are frequently based on 19th century taxonomic treatises or expedition reports, which do not lend themselves to quantitative interpretation. Although the use of presence–absence data overemphasizes the importance of rare species in assemblages, their employment is an inevitable consequence of large-scale analyses. Truly quantitative assessments of zoogeographic affinities of large pelagic organisms are recent and are restricted to a few oceanic provinces or to a few species (Barange *et al.* 1992; Gibbons, 1997; Gibbons and Thibault-Botha, 2002). The quality and originality of the proposed zoogeography in this paper rely on the use of a single instrument adapted to record the vertical distribution of fragile organisms in the upper kilometre of the ocean. The occurrence of several of these groups has been poorly documented using trawls and nets.

### Possible biases to the observed zoogeography

Three methodological biases can affect the zoogeography of mid-water zooplankton proposed in our analysis. First, the 12 cruises were conducted in different years and in different seasons. Consequently, the differences among the regions could result from temporal rather than spatial variability in the mesopelagic community composition. However, in two regions (MEDI and NAST), the profiles were performed in different seasons, allowing the quantification of temporal variability (Table 1). The MDS figure shows that all the profiles in the MEDI and NAST regions are grouped by provinces in two different areas of the MDS projection, suggesting that the seasonal differences are smaller than regional ones. Second, the level of similarity among stations may be affected by the number and level of taxa that can be recognized. An example is given by comparing the present spatial distribution

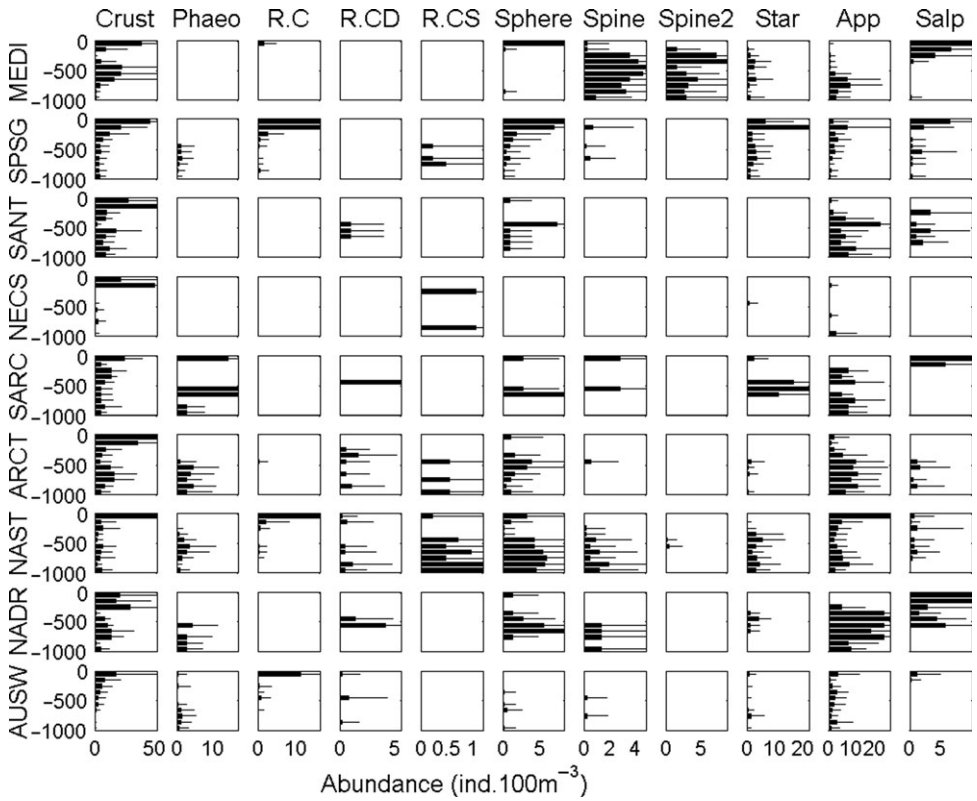


**Figure 9.** Vertical distribution of macrozooplankton in the different water masses. Average abundance (horizontal bars) and standard deviation (error bars) are noted for the following groups: crustaceans (Crust.), Phaeodarians (Phaeo.), colonial radiolarians of different types (R.C., R.CD., and R.CS.), spheres, single-cell sarcodines of different types (Spine., Spine2., Star.), appendicularians (App.), Thaliacae (Thal.) in the nine regions (rows).

in the North Atlantic with the previous work of Stemmann *et al.* (2008). The present results for the North Atlantic, based on 21 taxonomic groups and using additional data from the POMME cruise, confirm the previous distinction between the SARC–NAST and the ARCT–NAST regions, but they differ for the comparison between SARC and ARCT regions. The latter were significantly different in Stemmann *et al.* (2008), whereas no significant difference was observed in this study (Table 2). The discrepancy between the present analysis and the previous analysis of Stemmann *et al.* (2008) may arise from the addition of nine taxonomic groups (mainly subgroups of sarcodines) that had a similar distribution in both regions, contributing to an increase in the similarity (Figures 5, 8, and 9). Third, the relatively large within-region variability observed in the MDS plot (Figure 6) may be caused by the small number of individuals in several taxa that impart a high variability in the calculation of Bray–Curtis distances (notably SPSG, MEDI, NECS, and AUSW).

## UVP zoogeography

The regions defined in the present work correspond to nine of the biogeochemical provinces of Longhurst (1998). Despite the possible biases, the MDS plot indicates a consistent pattern in the spatial distribution of the communities in the main oceanic regions (MEDI, AUSW, NECS, ARCT, and SPSG), and the ANOSIM test reveals that all comparisons between regions, but two, were significantly different (Table 2). The two cases with similar composition in the macrozooplankton communities were adjacent regions in the highly dynamic environment of the North Atlantic SPF. These results suggest that the mesopelagic macrozooplankton community may be structured at the basin scale, but not at smaller scale such as oceanic front.

The analysis of the most abundant groups within each region reveals that the main difference between regions is the decreased proportion of all gelatinous carnivores and chaetognaths from 95% to 15% from the high-latitude regions (NECS, ARCT, NADR, SARC, and SANT; Figure 5) to the low-latitude regions (MEDI, AUSW, and SPSG). Therefore, the proposed zoogeography could be interpreted as resulting from a balance between the abundance of gelatinous predators and the other organisms. Therefore, the zoogeography that we propose in this work is related more to the function or the trophic status than the taxonomy. More study, however, is required to verify if the observed patterns in the mesopelagic layers are global.

## UVP zoogeography compared with previous work

The comparison of the zoogeography inferred from the UVP results and previous studies is difficult for two reasons. First, the UVP allows a detailed recognition to the genus or species level for only a limited number of organisms. Second, to our knowledge, no studies have attempted to define the mesopelagic zoogeography of zooplankton over such large spatial scales and used a consistent method for the quantification of a relatively large number of taxonomic groups.

Quantitative zooplankton zoogeography has been put forward for different oceanic basins. The most complete proposal deals with epipelagic copepods in the North Atlantic (Beaugrand and

Ibanez, 2002). The assemblages of calanoid copepods were grouped in four regions: the SPF (which corresponds roughly to NADR), the Subtropical Gyre (which corresponds roughly to NAST), the Arctic region (an area west of the region north of the SPF that corresponds approximately to ARCT), and the Subarctic region (an area east of the region north of the SPF that corresponds approximately to SARC). These divisions correspond roughly to the locations of three regions revealed as different in this paper for the mesopelagic communities (ARCT vs. NAST, NAST vs. NADR, ARCT vs. NADR; Table 2). In contrast to the results of Beaugrand and Ibanez (2002) for epipelagic copepods, the macrozooplankton community in the SARC region is not significantly different from the ARCT and the NADR regions (Table 2). The lack of significant differences in the macrozooplankton composition in these three mesopelagic regions may be because they were contiguous, and environmental conditions (e.g. temperature and particle content) were similar and stable enough that the community composition of the living fauna varied little.

### Comparisons with previous work for selected groups

Comparisons with previous studies can be done for four groups of medusae. *Solmundella bitentaculata* is usually found between 100 and 500 m in the Atlantic, Pacific, and Indian oceans, as well as in the Mediterranean Sea. This species is particularly common in the southern hemisphere (Shepherd and Thomas, 1982; O'Sullivan, 1984; Gili *et al.*, 1998). Our results are consistent with these observations because *S. bitentaculata* was found in five regions (except MEDI, NECS, SARC, and AUSW) with the greatest abundances in the southern hemisphere stations (SPSG and SANT; Figures 7 and 8). Medusae of the genus *Haliscera* have been reported in the mesopelagic and bathypelagic layers of the North Atlantic, Arctic, and Pacific oceans, and in the Adriatic Sea (Kramp, 1959; Gili *et al.*, 1998; Benovic *et al.*, 2005). We found this group in the North Atlantic, South Pacific, and Subantarctic oceans, but not in the MEDI, SARC, and AUSW regions (Figure 8). The discrepancy between the present data and previous investigations may be caused by the low abundances of this group (11 individuals were detected; Figure 4). *Aglantha* spp. are very common in the North Atlantic, from $\sim$35°N to the Arctic Ocean and also in the North Pacific (Gili *et al.*, 1998). They were only present in the North Atlantic, north of 35°N in our dataset, in agreement with the previous findings (Figure 8). *Aeginura grimaldi* has been reported in the Atlantic and Pacific oceans (Gili *et al.*, 1998). This species was only found in the Atlantic Ocean in our surveys (Figure 8).

Among the sarcodines, Phaeodarians constitute a group of radiolarians that has been poorly studied [see Paterson *et al.* (2007) for a review]. They occur in the mesopelagic layer, mostly in the Pacific and Antarctic oceans, but they also appear in the North Atlantic. In our dataset, Phaeodarians were found below 500-m depth in all the regions except the MEDI, SANT, and NECS (Figure 9). Their greatest concentrations were observed in the Atlantic Ocean (up to 10% of the total count in the SARC) in areas where, to our knowledge, they had never been reported before, suggesting that an important component of the midwater community has been overlooked. Also, large colonial radiolarians have not been studied sufficiently because many colonies lack siliceous skeletons and are easily destroyed in nets (Dennett *et al.*, 2002). However, they are an important component of the epipelagic ecosystem, because they host symbionts capable of primary production. Colonial radiolarians were abundant in the upper 150 m of the central North Pacific Ocean, with concentrations ranging from 2.8 to 43.3 colonies $m^{-3}$ ($\sim$10 colonies $m^{-3}$ on average; Dennett *et al.*, 2002). In the South Pacific Gyre, we recorded lower concentrations ranging from 0.05 to 0.9 colonies $m^{-3}$ in the upper 100 m ($\sim$0.5 colonies $m^{-3}$ on average). The difference in the estimates may be caused by the video plankton recorder detecting smaller objects ($<$1 cm) than the UVP used in this study. However, in both central Pacific ecosystems, colonial radiolarians were numerous.

Appendicularians constitute another taxonomic group that has received insufficient study in the mesopelagic realm. In the epipelagic layers, they are one of the most common members of the zooplankton community, often the second most abundant group after copepods (Gorsky and Fenaux, 1998). In the mesopelagic layer, appendicularians have been reported in many studies, but their quantitative importance is poorly known (Davoll and Youngbluth, 1990; Hopcroft and Robison, 2005). The present work demonstrates that this group is abundant in the deep waters of all the oceanic regions, constituting on average 13% of the total macrozooplankton population (30% in the SANT region; Figure 5). They often form peaks in abundance below 400-m depth (up to 58 ind. 100 $m^{-3}$; Figure 9).

## Conclusions and perspectives

The UVP imaging system collects less taxonomically specific data than towed nets, but provides a more rapid and less invasive means of obtaining quantitative estimates of the vertical distribution and abundance of macrozooplankton. The UVP has been used in nine oceanic regions of the ocean that corresponded to nine of the biogeochemical provinces of Longhurst (1998). The composition of macrozooplankton communities in the depth layers between 100 and 1000 m was different in the all regional comparisons but two, which corresponded to adjacent regions of the North Atlantic Ocean. These results suggest the mesopelagic macrozooplankton community is structured at the global scale, but not necessarily at the smaller scales such as oceanic frontal systems.

## Acknowledgements

We thank the crew of the different research vessels for their valuable assistance and support. The manuscript was improved by valuable comments from two anonymous reviewers. This research was co-funded by the MARECO programme in the framework of CENSUS of Marine Life project, the Australian Southern Surveyor voyage SS200605, EC Contract No. GOCE-036949 by the European Commission's Sixth Framework Programme under the priority "Sustainable Development, Global Change and Ecosystems", the French PROOF programme, and the ZOOPNEC programme component of the French programme. Funding to pay the Open Access publication charges for this article was provided by EC Contract No. GOCE-036949, the European Commission's Sixth Framework Programme under the priority "Sustainable Development, Global Change and Ecosystems".

## References

Barange, M., Pillar, S. C., and Hutchings, L. 1992. Major pelagic borders of the Benguela upwelling system according to euphausiid species distribution. South African Journal of Marine Science, 12: 3–17.

Beaugrand, G., and Ibanez, F. 2002. Spatial dependence of calanoid copepod diversity in the North Atlantic Ocean. Marine Ecology Progress Series, 232: 197–211.

Benovic, A., Davor, L., Onofri, V., Batistic, M., and Njire, J. 2005. Bathymetric distribution of medusae in the open waters of the middle and south Adriatic Sea during spring 2002. Journal of Plankton Research, 27: 79–89.

Clarke, K. R., and Warwick, R. M. 2001. A further biodiversity index applicable to species lists: variation in taxonomic distinctness. Marine Ecology Progress Series, 216: 265–278.

Davoll, P. J., and Youngbluth, M. J. 1990. Heterotrophic activity on appendicularian (Tunicata: Appendicularia) houses in mesopelagic regions and their potential contribution to carbon flux. Deep Sea Research, 37: 285–294.

Dennett, M. R., Caron, D. A., Michaels, A. F., Gallager, S. M., and Davis, C. S. 2002. Video plankton recorder reveals high abundances of colonial Radiolaria in surface waters of the central North Pacific. Journal of Plankton Research, 24: 797–805.

Gibbons, M. J. 1997. Pelagic biogeography of the South Atlantic Ocean. Marine Biology, 129: 757–768.

Gibbons, M. J., and Thibault-Botha, D. 2002. The match between ocean circulation and zoogeography of epipelagic siphonophores around southern Africa. Journal of the Marine Biological Association of the UK, 82: 801–810.

Gili, J-M., Bouillon, J., Pagès, F., Palanques, A., Puig, P., and Heussner, S. 1998. Origin and biogeography of the deep-water Mediterranean hydromedusae including the description of two new species collected in submarine canyons of northwestern Mediterranean. Scientia Marina, 62: 113–134.

Gorsky, G., and Fenaux, R. 1998. The role of Appendicularia in marine food webs. *In* The Biology of Pelagic Tunicates, pp. 161–169. Ed. by Q. Bone. Oxford University Press, Oxford.

Gorsky, G., Flood, P. R., Youngbluth, M., Picheral, M., and Grisoni, J. M. 2000. Zooplankton distribution in four western Norwegian fjords. Estuarine Coastal and Shelf Science, 50: 129–135.

Haeckel, E. 1887. Report on the Radiolaria collected by HMS. Challenger during the Years 1873–76. Zoology XVIII (Part I).

Hopcroft, R., and Robison, B. 2005. New mesopelagic larvaceans in the genus Fritillaria from Monterey Bay, California. Journal of the Marine Biological Association of the UK, 85: 665–678.

Kramp, P. L. 1959. The hydromedusae of the Atlantic Ocean and adjacent waters. Dana Reports, 46: 1–283.

Legendre, P., and Legendre, L. 1998. Numerical Ecology. Elsevier Science Publishers, Amsterdam.

Lindsay, D. J., Furushima, Y., Miyake, H., Kitamura, M., and Hunt, J. C. 2004. The scyphomedusan fauna of the Japan Trench: preliminary results from a remotely-operated vehicle. Hydrobiologia, 530–531: 537–547.

Lindsay, D. J., and Hunt, J. C. 2005. Biodiversity in midwater cnidarians and ctenophores: submersible-based results from deep-water bays in the Japan Sea and northwestern Pacific. Journal of the Marine Biological Association of the UK, 85: 503–517.

Longhurst, A. R. 1998. Ecological Geography of the Sea. Academic Press, London. 398 pp.

O'Sullivan, D. 1984. Guide to the Hydromedusae of the Southern Ocean and Adjacent Waters. ANARE Research Notes 5 (Australian National Antarctic Research Expedition). Australia Dept of Science and Technology, Antarctic Division, Tasmania, Kingston, Australia.

Paterson, H. L., Pesant, P., Cloded, P., Knotta, B., and Waite, A. M. 2007. Systematics of a rare radiolarian: *Coelodiceras spinosum* Haecker (Sarcodina: Actinopoda: Phaeodaria: Coelodendridae). Deep Sea Research Part II—Topical Studies in Oceanography, 54: 1094–1102.

Perry, R. I., and Smith, S. J. 1994. Identifying habitat associations of marine fishes using survey data—an application to the Northwest Atlantic. Canadian Journal of Fisheries and Aquatic Sciences, 51: 589–602.

Raskoff, K. A. 2001. The impact of *El Niño* events on populations of mesopelagic hydromedusae. Hydrobiologia, 451: 121–129.

Robison, B. H. 2004. Deep pelagic biology. Journal of Experimental Marine Biology and Ecology, 300: 253–272.

Shepherd, S. A., and Thomas, I. M. 1982. Marine Invertebrates of Southern Australia Part I. *In* Handbook of the Flora and Fauna of South Australia. Ed. by D. J. Woolman. Government Printer, Adelaide.

Stemmann, L., Hosia, A., Youngbluth, M. J., Picheral, M., and Gorsky, G. 2008. Vertical distribution (0–1000 m) of macrozooplankton, estimated using the underwater video profiler, in different hydrographic regimes along the northern portion of the Mid-Atlantic Ridge. Deep Sea Research II, 70: 94–105.

Vinogradov, G. M. 2005. Vertical distribution of macroplankton at the Charlie-Gibbs Fracture Zone (North Atlantic), as observed from the manned submersible "Mir-1". Marine Biology, 146: 325–331.

doi:10.1093/icesjms/fsn010